

EDGAR: An Autonomous Driving Research Platform - From Feature Development to Real-World Application

Journal Title
XX(X):1–16
©The Author(s) 2016
Reprints and permission:
sagepub.co.uk/journalsPermissions.nav
DOI: 10.1177/ToBeAssigned
www.sagepub.com/

SAGE

Phillip Karle¹, Tobias Betz¹, Marcin Bosk², Felix Fent¹, Nils Gehrke¹, Maximilian Geisslinger¹, Luis Gressenbuch³, Philipp Hafemann¹, Sebastian Huber¹, Maximilian Hübner⁴, Sebastian Huch¹, Gemb Kaljavesi¹, Tobias Kerbl¹, Dominik Kulmer¹, Tobias Mascetta³, Sebastian Maierhofer³, Florian Pfab¹, Filip Rezabek⁵, Esteban Rivera¹, Simon Sagmeister¹, Leander Seidlitz⁵, Florian Sauerbeck¹, Ilir Tahiraj¹, Rainer Trauth¹, Nico Uhlemann¹, Gerald Würsching³, Baha Zarrouki¹, Matthias Althoff³, Johannes Betz⁶, Klaus Bengler⁴, Georg Carle⁵, Frank Diermeyer¹, Jörg Ott², and Markus Lienkamp¹

Abstract

While current research and development of autonomous driving primarily focuses on developing new features and algorithms, the transfer from isolated software components into an entire software stack has been covered sparsely. Besides that, due to the complexity of autonomous software stacks and public road traffic, the optimal validation of entire stacks is an open research problem. Our paper targets these two aspects. We present our autonomous research vehicle *EDGAR* and its digital twin, a detailed virtual duplication of the vehicle. While the vehicle's setup is closely related to the state of the art, its virtual duplication is a valuable contribution as it is crucial for a consistent validation process from simulation to real-world tests. In addition, different development teams can work with the same model, making integration and testing of software stacks much easier, significantly accelerating the development process. The real and virtual vehicles are embedded in a comprehensive development environment, which is also introduced. All parameters of the digital twin are provided open-source at https://github.com/TUMFTM/edgar_digital_twin.

Keywords

Autonomous Vehicles, Digital Twin, Data Mining, Hardware-in-the-Loop

1 Introduction

Autonomous software stacks must comprise a broad range of features to enter the complex environment of public road traffic. The two major challenges from feature development to real-world application of these stacks are an efficient, early integration of isolated software components into an overall software stack and the optimal and complete validation of this full stack. A holistic simulation environment is a crucial aspect to solve these challenges. This is due to the big variety of scenarios (Li and Zhai 2019), which require reproducible and easily scalable virtual testing to reduce the effort of real-world tests. In addition, with a shared virtual development environment, the integration effort is facilitated. However, with available simulation platforms for autonomous vehicles (AV), there is a significant inconsistency between virtual and real-world tests because different models are used. Thus, a digital twin, a virtual representation of the physical entity able to simulate the system's lifecycle (Souza et al. 2019), is indispensable to ensure the consistency and validity of the results. The consistency of vehicle dynamics, sensor behavior, and network properties are the essential factors for this use case. As Tao et al. (Tao et al. 2019) even state, creating a digital twin is one of the major challenges in the research and improvement of autonomous vehicles.

The research platform presented in this paper targets this aspect: We propose our research vehicle called *EDGAR*

(Excellent Driving GARching, Fig. 1) and its digital twin, a detailed virtual duplication. In summary, the main contributions of this paper are:

- We propose an autonomous research vehicle with a multi-sensor setup and different computing hardware architectures (x86, ARM) that addresses multiple

All authors are with Technical University of Munich, Garching, GER
¹School of Engineering and Design, Department of Mobility Systems Engineering, Institute of Automotive Technology and Munich Institute of Robotics and Machine Intelligence (MIRMI)
²School of Computation, Information and Technology, Department of Computer Engineering, Chair of Connected Mobility
³School of Computation, Information and Technology, Department of Computer Engineering, Professorship Cyber-Physical Systems
⁴School of Engineering and Design, Department of Mechanical Engineering, Chair of Ergonomics
⁵School of Computation, Information and Technology, Department of Computer Engineering, Chair of Network Architectures and Services
⁶ School of Engineering and Design, Department of Mobility Systems Engineering, Professorship Autonomous Vehicle Systems and Munich Institute of Robotics and Machine Intelligence (MIRMI)

Corresponding author:

Phillip Karle, Institute of Automotive Technology, Munich Institute of Robotics and Machine Intelligence (MIRMI), Technical University of Munich, 85748 Garching, GER.
Email: phillip.karle@tum.de



Figure 1. EDGAR: The research vehicle of the Technical University of Munich.

research topics (perception, planning, control, teleoperation, HMI, network communication, V2X).

- We present a comprehensive digital twin with vehicle dynamics models and sensor and network replication for a consistent testing strategy from simulation to reality. The digital twin setup is available open-source. To the best of our knowledge, this is the first publicly available digital twin of an autonomous road vehicle.
- We introduce a holistic workflow starting from feature development over multiple simulation steps to real-world testing in which the real and virtual vehicles are embedded. In addition, the development environment offers a large-scale data center for systematic data handling of stored sensor data and software logs to foster software development.

2 Related Work

The following section covers the related work of AV development systems. These systems comprise research vehicles for real-world testing and data recording and evaluation processes. For a general survey about the state of the art of hardware and software for AVs, we refer to (Yurtsever et al. 2020; Badue et al. 2021).

Since the 1980s, prototypical vehicles have been set up to demonstrate the capabilities of autonomous systems in real-world traffic (Dickmanns 2002). Among these are Alvin (Pomerleau 1988), a camera-end-to-end single-lane following vehicle, VaMoRs (Maurer et al. 1995), a computer vision-based vehicle for lateral and longitudinal guidance, Prometheus (Williams 1988) with a 4D-based approach of image-processing. Fig. 2 shows some of these iconic cars. Based on these milestones, Table 1 outlines research vehicle platforms. It can be observed that most work on AV research vehicles focuses on the real vehicle setup, including sensors and computing platforms. None of them offers a digital twin of the presented vehicle.

Several works focus on the requirements for an AV sensor setup (Broggi et al. 2010; Chen et al. 2012) and how to fulfill them (Cho et al. 2014; Van Brummelen et al. 2018; Leonard et al. 2008; Taraba et al. 2018; Campbell et al. 2018; Furgale et al. 2013). Furthermore, various research institutions use vehicles with sensors and computation hardware to gather data from road scenarios (Geyer et al. 2020; Ligocki et al.

2020; Burnett et al. 2022; Carballo et al. 2020). Since these vehicles are not used for testing and evaluating self-driving software, we are not going into further detail here.

A reliable development workflow is required to test and validate the developed AV features. A common approach is to start on the feature and module level with unit tests and Model-in-the-Loop (MiL), followed by overall software tests in Software-in-the-Loop (SiL-) and Hardware-in-the-Loop (HiL-) simulations. Afterward, the real-world tests are the final stage to validate the software. Gao et al. (Gao et al. 2022) propose such an evaluation system and provide an overview of the required infrastructure and methods for this system. They name four major research directions to focus on: Virtual reality-based driving scenarios, automated safety scenario validation, trustworthy machine learning analysis methods, and system security evaluation models. Thorn et al. (Thorn et al. 2018) present a scenario-based test framework for automated driving functions of SAE Level 3-5 (SAE 2021). In addition, fail-operational and fail-safe strategies are identified for the investigated AV systems. Similarly, Chakra (Chakra 2022) analyses the sim2real-gap for resilient real-world applications. He states the three main areas for future research: The definition and measurement of AV intelligence, the general enhancement in AV simulation frameworks and methodologies, and AV simulation transferability and integration. With a focus on real-time capability and hardware constraints for mobile applications, Lin et al. (Lin et al. 2018) present and formalize a design guideline. However, there is no analysis of the AV software features. A practical framework for an architecture design of software and hardware to create an overall AV system is shown by Zong et al. (Zong et al. 2018). Their contributions are comparing different sensor setups, a complete autonomous software validated in real-world applications, and new scalable data transmission systems.

The evaluation and testing process can also be bi-directional, i.e., during the evaluation and testing process, new development requirements and data for feature development can be derived. The extraction of information from real-world tests for further feature development is demonstrated by Liu et al. (Liu et al. 2020). The proposed pipeline uses logs from real-world tests for software feature development. They focus their development pipeline on self-adaptive path planning. The proposed planning algorithm is able to improve its knowledge base of collision scenarios after a test is performed and thereby avoids dangerous situations that might occur during testing in the future. In contrast, Deliparaschos et al. (Deliparaschos et al. 2020) propose to derive data from sensors placed on the road infrastructure to extract driving scenarios for model verification and validation. Zhao et al. (Zhao and Peng 2017) extend the idea of real-world data collection by data augmentation. They propose to collect data from real-world driving, focusing on real-world edge case scenarios, i.e., meaningful and safety-critical scenarios. A Monte Carlo simulation is applied to these scenarios for higher complexity. Subsequently, the simulation enables us to derive a statistical analysis of how the AV would perform in everyday driving conditions. The authors conclude that by means of this method, the real-world effort can be reduced



Figure 2. Milestones of AV research vehicles: VaMoRs (Maurer et al. 1995), Stanley (Thrun et al. 2006), Boss (Urmson et al. 2008), MB S-Class (Ziegler et al. 2014)

Table 1. Overview of the state of the art of AV research vehicles.

	Environment Sensors			Computing Platform			Digital Twin		
	Camera	LiDAR	RADAR	PC	Real-Time	GPU	Sensors	Vehicle Dynamics	Network
Stanley ¹	1	5	2	✓					
Junior ²	0	8	5	✓					
Boss ³	2	11	5	✓					
Bertha ⁴	3	0	8		-				
Braive ⁵	10	5	0	✓					
CMU vehicle ⁶	2	6	6	✓		✓			
Fortuna ⁷	5	3	4	✓	✓	✓			
Jupiter ⁸	1	3		✓	✓				
X-Car ⁹	7	1	1	✓		✓			
EDGAR (ours)	10	4	6	x86, ARM	ARM	✓	✓	✓	✓

significantly, but the variety of scenarios remains high due to the synthetic augmentation.

Regarding the quantification of the test effort, Hauer et al. (Hauer et al. 2019) propose a method to determine if an AV system is tested in all scenarios, i.e., if sufficient real drive data is collected. Using the Coupon Collector’s problem, a statistical guarantee can be given that all scenario types are covered. The standardization of AV performance evaluation is the focus of the work of Basantis et al. (Basantis et al. 2019). They conclude that standardized testing can be a valuable tool to evaluate the capabilities of AV vehicles and that a robust evaluation mechanism might have a big impact on the conformance of AV systems.

In summary, the presented work on AV research vehicles either focuses on the hardware setup or states the deployment method for the software without validation. The work in the field of AV evaluation and development systems is mainly conceptual, i.e., only requirements are identified for AV software validation. Even though the process to base feature development on test data is introduced in the state of the art, the implementation of an AV validation concept in an overall software development workflow is sparsely covered, e.g., by (Thorn et al. 2018). The consideration of a digital twin, which connects the real-world system with the virtual one and thus ensures the consistency and validity of the entire process, is completely neglected.

We aim to establish this consistency with our research vehicle *EDGAR* and its digital twin, embedded in our proposed workflow from feature development to real-world application. In the scope of this work, a detailed introduction of the hardware setup of our AV research vehicle is given. The related digital twin comprises vehicle dynamic models and sensor and network replication, which are also presented. Our development workflow comprises the forward step from feature development via multi-stage testing and validation to real-world application and the backward step to use the

real-world data for the improvement of the simulation and to derive new feature requests.

3 Autonomous Vehicle Setup

The hardware setup of *EDGAR* is described in the following section. Starting with the base vehicle (3.1), we then introduce the sensors mounted on the vehicle (3.2) and the computer and network components (3.3). For each component, the design decisions from a technical point of view and the constraints for the final decision are described. The description of the actuation interfaces completes the overview of the vehicle hardware setup and the actuation interfaces (3.4). Finally, the HiL simulation framework (3.5) and the data center (3.6) are described. Table 2 lists all hardware components.

3.1 Vehicle

The Volkswagen T7 Multivan Style 1.4 eHybrid is a hybrid electric vehicle and provides the basis for the research vehicle *EDGAR*. One of the key advantages of using the T7 Multivan Style 1.4 eHybrid for autonomous driving research is its hybrid powertrain. The vehicle has a 1.4-liter turbocharged four-cylinder engine, an electric motor, and a 13 kWh lithium-ion battery. With an estimate of about 1.5 kW of continuous power, the vehicle’s alternator provides enough power to operate the prototype computers and sensors. Another benefit of the Volkswagen T7 is its advanced features, such as Adaptive Cruise Control, Lane Departure Warning, Park Assist, and Emergency Assist. These features provide safety-certified actuator interfaces that can be reused cost-effectively as a fallback for the developed software and comparison. In addition, the space inside is advantageous to place all components easily accessible in the trunk and to improve the airflow to cool them. A computer is placed between the two front seats with

two screens mounted inside the vehicle to visualize the state of the AV software and vehicle during test rides.

Despite the advantages of using the T7 Multivan Style 1.4 eHybrid as a research platform, there are also some limitations to consider. The vehicle is relatively large, which can make it less suitable for testing in densely populated urban areas. The vehicle's height especially poses difficulties in sensor placement, with a trade-off between near-field coverage and a far-range sensor focus.

3.2 Sensors

Our sensor setup consists of cameras, LiDARs, RADARs, and microphones for the local environment perception. In addition, a GPS-IMU system is included. Two requirements that apply to the whole sensor setup are:

- Precision Time Protocol (PTP) capability for time synchronization inside the car
- ROS2-compatible drivers for software integration

Further requirements, intended use cases, and final choice for each sensor are discussed in the following subsections.

The described setup enables a holistic coverage with camera, RADAR, and LiDAR sensors. Fig. 3 depicts a front view of the sensor roof rack showing the front LiDARs and cameras, and Fig. 4 shows the field of view of the perception sensors. The detailed positions and orientations

Table 2. Overview of the hardware components (MR: Mid-Range, LR: Long-Range, GM: Grandmaster).

Component	Producer	Model
Series vehicle	Volkswagen	T7 Multivan 1.4 eHybrid
Mono camera	Basler	acA1920-50gc
Stereo camera	Framos	D455e
LiDAR MR	Ouster	Ouster OS1-128
LiDAR LR	Innovusion	Falcon Gen-2
RADAR	Continental	ARS430
GPS-IMU	Novatel	PwrPak7D-E2
Microphones	Infineon	A2B Eval Kit
x86 HPC	InoNet	Mayflower B17
ARM HPC	ADLINK	AVA AP1
Network Switch	Netgear	M4250-40G8XF-PoE+
PTP GM	Masterclock	GMR5000
SDR Transceiver	Ettus	USRP B210 SDR Kit 2x2
V2X System	Cohda	MK5 OBU
5G-Router	Milesight	UR75-500GL-G-P-W
MIMO Antennas	Panorama	LGMQM4-6-60-24-58 4x4
LED	BTF lighting	WS2815
LED controller	Strip Studio	SPI Matrix
Visualization PC	Spo-comm	RUGGED GTX 1050 Ti

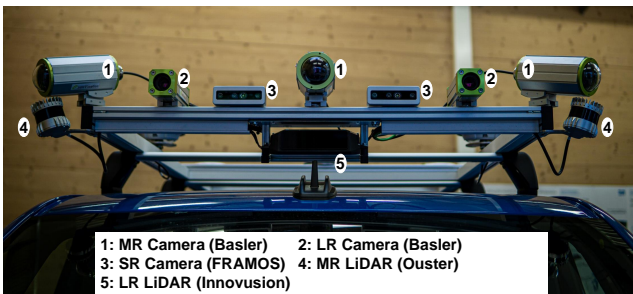


Figure 3. Front roof area with LiDAR and Camera sensors (MR: Mid-Range, LR: Long-Range, SR: Short-Range).

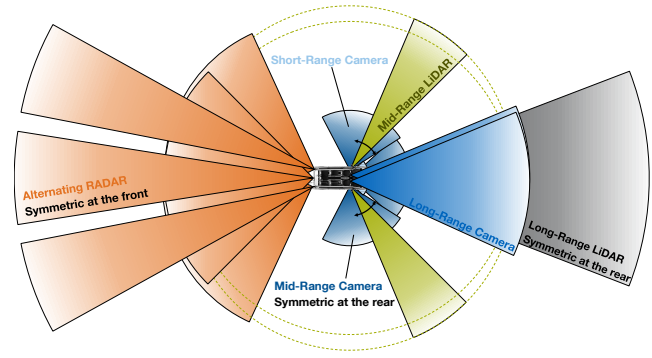


Figure 4. Field of view of the perception sensors.

of the sensors are given in the repository of the digital twin. All positions and orientations are stored in a .urdf-file. The reference point is the middle of the rear axle.

3.2.1 Camera The camera setup of the research vehicle was designed with two applications in mind: Autonomous driving and teleoperation of the vehicle. For these two applications, the following requirements were identified:

- 360° Field-of-View (FOV);
- a minimal resolution of 1280 x 720 pixel;
- a frame rate of 40 fps to minimize the latency;
- a consistent camera-lens combination to simplify stitching the camera images; and
- the option for depth completion through stereo cameras.

Mid-Range: To fulfill these criteria, we chose 6 Basler acA1920-50gc cameras with the Sony IMX174 CMOS sensor for a 360° representation with mono camera images. These cameras are capable of providing FullHD (1920 x 1200 pixel) color images at a maximum frame rate of 50 Hz. Three cameras are mounted on the front center and corners of the vehicle's roof. Combined with lenses with a focal length of 6 mm (Kowa LM6HC), each front camera provides a horizontal FOV of 84.9° and a vertical FOV of 59.7°. At the rear end of the vehicle's roof, three cameras are mounted in combination with a Kowa LM4HC lens, having a focal length of 4.7 mm. The resulting FOVs (horizontal: 99.5°, vertical 73.1°) ensures in a small blind spot at the vehicle's sides.

Long-Range: Two additional Basler acA1920-50gc cameras are mounted at the front of the vehicle. These cameras are combined with lenses having a focal length of 16 mm, resulting in a horizontal FOV of 38.6° and a vertical FOV of 24.8°. The purpose of these cameras is to provide stereovision and far-range vision.

Short-Range: Two FRAMOS D455E depth cameras are attached to the vehicle's roof rack. These cameras make use of the active IR Stereo technology and provide depth images with a maximal resolution of 1280 x 720 pixels at a maximal framerate of 30 Hz.

3.2.2 LiDAR The LiDAR setup was designed to enable autonomous driving in arbitrary traffic scenarios (i.e., urban and highway settings). In summary, our requirements were the following:

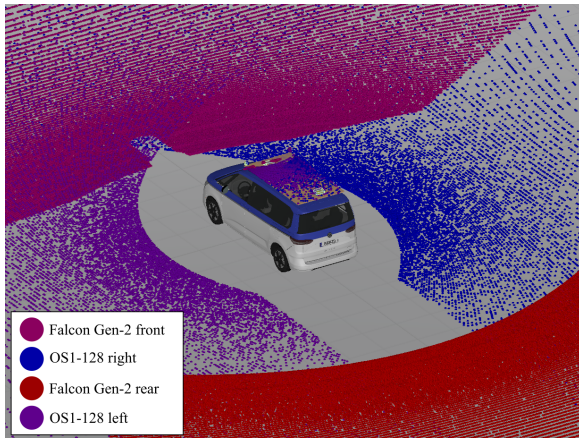


Figure 5. Unity environment to simulate point clouds for different LiDAR configurations.

- 360° FOV with blind spots as small as possible directly around the vehicle;
- high range, especially to the front and rear; and
- dense reflections in close and mid-range.

For the selection process of a LiDAR setup, we created a simulation environment based on *Unity* to generate synthetic point clouds with different setups. The simulation was based on (Betz et al. 2023a) and adapted to the new base vehicle. An exemplary simulation of a LiDAR setup is shown in Fig. 5. It can be seen that a setup of four LiDAR sensors satisfies our needs of minimized blind spots around both sides of the car but a high perception range to the front and rear best. Two rotating sensors are placed on the left and right front corners of the vehicle roof. Two long-range solid-state LiDARs are placed at the front and rear center of the rooftop.

Mid-Range: For short- and mid-range detections, two Ouster OS1-128 were chosen. Those are rotating 360° sensors with a vertical FOV of 45° with higher resolution in the center of the vertical FOV. They offer a range of 45 m at 10 % reflectivity using a 865 nm wavelength laser.

Long-Range: To cover the most important regions around the vehicle, namely front and rear, two additional LiDARs were added to the corresponding centers of the roof. These put more focus on long-range detections. The therefore chosen Innovusion Falcon offer a range of 250 m at 10 % reflectivity through 1550 nm laser. They have a FOV of 120° horizontally and 25° vertically. Since the scan pattern of these LiDARs is software-defined, regions of interest (ROI) can be defined at runtime to locally increase the resolution.

3.2.3 RADAR In addition to LiDAR and camera, we also use RADAR sensors because of their high robustness against severe weather conditions and their ability to measure the velocity of the target objects. The sensors are used for RADAR-only detection and fusion algorithms, e.g., Camera-RADAR-Fusion. The requirements to choose an appropriate sensor were the following:

- High detection range for long-range perception compared with a broad horizontal field of view for short-range perception;
- accurate measure of the velocity of target objects;
- high point cloud density; and
- 3D-detection, incl. elevation measurement.

Based on these requirements, our research vehicle's final choice is the Continental ARS430 radar sensor. Six of them are mounted on the vehicle in total. These pulse compression radar modulation sensors operate in the 77 GHz frequency band and alternate between a far and a near field scanning pattern, with a horizontal field of view of $\pm 9^\circ$ and $\pm 60^\circ$, respectively. The sensors have a maximum detection range of 250 m and an azimuth angular resolution of 0.1° . The radar sensors can measure the velocity of target objects with an accuracy of 0.1 km h^{-1} and detect objects up to a minimum radar cross section (RCS) of 10 m^2 (at a range of 200 m). In our case, the sensor has primarily been selected due to its ability to output data in a point cloud format and its information density (high number of output points). Finally, the possibility for PTP time synchronization and the integration into a ROS2 framework were two other important decision criteria. In contrast, the sensor misses the ability to measure elevation information and is limited to a 100 Mbit s^{-1} BroadR-Reach Ethernet connection, which restricts the number of output points.

3.2.4 GPS-IMU A Global Navigation Satellite System (GNSS) system is used to locate the research vehicle globally. The following requirements were identified:

- Combined system of GNSS and Inertial Navigation System (INS);
- support of Real-Time Kinematic (RTK); and
- measurement of vehicle heading at standstill.

Based on these requirements, we decided to use the NovAtel PwrPak7D-E2, a combined GPS-IMU system. The device supports Real-Time Kinematic (RTK) (Hatch 1991), which allows receiving GNSS correction data over the Internet. As a result, it allows us to determine the vehicle's current location with an accuracy of 2 cm on average*. Furthermore, it can measure the vehicle's current heading at standstill by using two NovAtel GNSS-850 antennas. This is essential if the autonomous vehicle intends to start driving autonomously after being booted. The integrated Inertial Measurement Unit (IMU) is used to derive the vehicle's dynamic state during a GNSS outage until the vehicle can do a safe stop. One disadvantage of the PwrPak7D-E2 is that it does not support PTP yet. As a result, the Pulse-per-Second (PPS) output of the system must be used for time synchronization*.

3.2.5 Microphones While most autonomous research vehicles only use cameras, RADAR, and LiDAR sensors for their perception pipeline, we decided to also use microphones. This enables further use cases like detection and localization of emergency vehicle sirens, blind spot detection, and road surface type estimation (Siwek 2021). Our most important requirements are:

- High fidelity;
- resistance to adverse environmental conditions;
- small physical dimensions; and
- low power consumption.

*<https://hexagondownloads.blob.core.windows.net/public/Novatel/assets/Documents/Papers/PwrPak7D-E2-Product-Sheet/PwrPak7D-E2-Product-Sheet.pdf>

The XENSIV™ IM67D130A MEMS microphones from Infineon Technologies offer a signal-to-noise ratio (SNR) ≥ 67 dB for improved audio quality and an acoustic-overload-point (AOP) ≥ 130 dB for high wind-noise robustness. Their housing is IP68-certified to protect the microphones from rain and dust. Infineon's A²B evaluation kit offers an AURIX microcontroller as an ECU master unit and four slave modules with four microphones each. The slave modules are attached to the vehicle corners and connected via A²B audio bus from Analog Devices.

The AURIX microcontroller can be flashed with custom code for audio preprocessing. It is connected to the HPC platform via Ethernet, where the detection and localization tasks can be executed.

3.3 Computer and Network

The computer and network system comprises two high-performance computers, a network switch, and a PTP grandmaster (GM), introduced in the following subsections.

3.3.1 High-Performance Computer The research vehicle is equipped with HPC platforms to handle the processing demands of the autonomous driving software. The HPC platforms should fulfill the following requirements:

- Multi-core (16) CPU with high clock frequency and large RAM for an overall low software latency (Betz et al. 2023b);
- a high GPU-capacity to run deep learning applications;
- a CAN interface to the vehicle actuators;
- a high network bandwidth to receive the sensor data; and
- a suitable storage setup for data recording.

In addition, we decided to operate two different HPC platforms based on the x86 and aarch64 architecture to compare their performance for autonomous driving systems. Based on the requirements, we chose two platforms: the x86-based InoNet Mayflower-B17 and the ARM-based ADLINK AVA AP1. The specifications are given in Table 3. A first evaluation of the x86-HPC processing power for Autware.Universe can be found in (Betz et al. 2023c). We deactivate the hyper-threading option at the x86-HPC, which leads to lower latencies in the software stack. Besides the selected GPUs, we integrate the FPGA-based development board AMD VCK5000, which enables fast AI inference. Both platforms have built-in connectivity options for communication, such as CAN interfaces to access the vehicle actuators. Since a large amount of data are recorded with the research vehicle, a so-called quick tray is available in the Mayflower-B17. This tray enables a fast change of the 4 x 2 TB NVMe SSDs. The AVA AP1 Platform features the integrated safety island, an additional high-safety, real-time capable CPU to execute safety-critical functions. The aforementioned architecture allows pursuing new research topics, such as developing safety features to ensure that the autonomous system can continue to operate even in the event of a component failure.

3.3.2 Network switch The network switch is a central component of the AV hardware setup. For the given use case, the following requirements were identified:

- Data transfer from all sensors (downlink)
- Data transfer to the HPCs (uplink) via Power-over-Ethernet (PoE)
- Audio-Video-Bridging (AVB) and IEEE 802.1Qav
- PTP compatibility

The chosen device, M4250-40G8XF-PoE+ by Netgear, fulfills these requirements. It offers 40 PoE+ ports and 8 SFP+ ports, which are patched to 2 x 40 Gbit s⁻¹ uplink, one for each HPC, and supports Audio Video Bridging (AVB), IEEE 802.1Qav, and additional Time-Sensitive Networking (TSN) standards. In addition, the network switch serves as a transparent clock in the cascaded PTP system, i.e., it modifies the PTP timestamp from the PTP GM based on its residence time.

3.3.3 PTP Clock Synchronization Time synchronization is essential in a system with multiple different and distributed sensors to record a high-quality data set without a time shift between individual sensors. Such capabilities are even more prominent when multiple vehicles exchange information and require freshness of the data. The requirements for this component are the following:

- PTP master functionality to adjust the system clocks of several PTP slaves in the network to keep them synchronized (IEEE 2020);
- time-synchronization with non-PTP-capable devices; and
- low clock drift.

PTP is organized in a master-slave hierarchy, where the slave device is always synchronizing its internal clock to the information provided by the master. For that, the PTP standard defines three clock types - boundary clock (BC), ordinary clock (OC), and transparent clock (TC). The OC has only a single port that is either in a master or slave state. On the other hand, the BC has two or more ports and is used to link complex PTP topologies. Last is the TC, which is not a master or slave and does not have an internal clock. TC forwards PTP messages, adjusts their time correction field according to the residence time, and improves the PTP synchronization precision (Rezabek et al. 2022b). On top of this hierarchy is the GM clock that determines the clock for the whole system.

For our setup, we chose the Masterclock GMR5000, a state of the art PTP GM clock. This allows maximum modularity and flexibility in switching components compared to a solution where, for example, the GNSS System would act as GM. Furthermore, the GMR5000 offers multiple interfaces for time-synchronization with non-PTP-capable devices (3.2.4), increasing the number of potentially usable system components and sensors.

The clock can be synchronized with the current GNSS time by connecting the GMR5000 to a GNSS antenna or receiving the PPS signal from the vehicle's GNSS system. The GMR5000 is equipped with an optional high-stability oscillator that lowers the time drift to about ± 0.25 s/year[†].

[†]<https://static1.squarespace.com/static/55f05c0ce4b03bbf99b13c15/t/5e8b6093a17e09405bb5e7ea/1586192532769/GMR5000+Data+Sheet.pdf>

Table 3. Specification of the vehicle computing platforms.

	InoNet Mayflower-B17	ADLINK AVA AP1
Architecture	x86	AArch64
CPU	AMD EPYC 7313P	Ampere Altra Q80-26
Cores/Threads	16/32	80/80
Clock Frequency	3.0 GHz (max 3.7 GHz)	2.6 GHz
RAM	4 x 32 GB DDR4	96 GB DDR4
Safety Island	–	NXP S32S247TV
Network Interface	SFP+ 4 x 10 Gbit s ⁻¹	
GPU	NVIDIA RTX A6000 48 GB	
Operating System	Ubuntu 22.04 Jammy Jellyfish	

Therefore, time offsets between GNSS time and the vehicle's time stay low which simplifies time synchronization during the boot phase of the car, especially after prolonged phases of vehicle shutdown. For the *EDGAR* vehicle, we do not need a clock synchronized to, e.g., GPS, but it is crucial to have such capabilities when the vehicle communicates to external parties.

To distribute the GM messages, we synchronize the Ego Vehicle (x86 HPC) with the GM. The x86 HPC serves as BC as it has multiple ports and allows for good interconnectivity. Besides, it is connected to the Netgear switch that runs in the TC mode and introduces less clock jitter. Therefore, there are only two hops from the x86 to the sensors. The sensors operate in the OC mode and listen to the clock information provided by the x86 HPC. We chose the x86 HPC as a master device for the sensors as it provides more granular control of the PTP configuration without sacrificing clock precision.

3.3.4 External Communication The design choices for our external communication system aim to increase usage flexibility, i.e., supporting different communication technologies. This includes software-defined radio (SDR) transceivers, a vehicle-to-everything (V2X) system, a router, and multiple-input multiple-output (MIMO) antennas.

SDR is a communication system where several parts of the communication functionality can be configured in software (Macedo et al. 2015). We integrated three Ettus USRP B210 SDR Kit transceivers. For communication with roadside infrastructure and other vehicles, we use the Cohda Wireless MK5 OBU[‡] V2X system, which supports the IEEE 802.11p V2X communication standard.

The vehicle's internet connection, which is received via 5G standard and allows communication to infrastructure, cloud-based computing, and teleoperation, is handled via the Milesight UR75-500GL-G-P-W industrial cellular 5G router. The high transmission rate of the 5G standard is especially important for teleoperation to ensure low latency and high bitrates. The router is equipped with dual SIM cards for backup between multiple carrier networks; the router supports PoE and has an integrated GPS module. As antennas, we selected the model LGMQM4-6-60-24-58 from Panorama Antennas, which support 3G, 4G, 5G, GPS, and WiFi. We integrated three of them to operate all three SDR transceivers independently. Furthermore, *EDGAR* has an additional coaxial connector on the roof to add further antennas for specific use cases.

3.4 Actuators

The interfaces between the AV HPCs and the series actuators are realized via CAN. A vehicle gateway serves as an API between the AV commands and the series communication interface.

In addition, LEDs are placed around the roof of the vehicle. These serve as external Human-Machine-Interface (eHMI) and are actuated via a USB-interface.

3.5 HiL simulator

A custom HiL simulator is built to enable quick development cycles, software optimization, and interface testing. Using the same hardware as deployed in the real vehicle is crucial, as it ensures comparability of the results generated in the HiL simulator and simple transferability of software modules to the real vehicle. The HiL setup comprises the same network router, switch, HPCs, and PTP GM (Fig. 9). Hence, the autonomy software on the HPCs can be evaluated, but it is also possible to prove the network setup and to run in teleoperated mode. To ensure consistency between simulation and real-world tests, our digital twin is embedded into the HiL-Simulation. Its specification is given in the repository, including vehicle parameters and sensor mounts.

The HiL simulator is primarily used for virtual validation tests before real-world tests. In addition, with the virtual sensor setup placed into the simulation, it is possible to evaluate the autonomous software performance with the same constraints of occlusions and limited resolutions as the real-world vehicle. Also, the sensor settings can be analyzed, adjusted, and transferred to the real-vehicle setup. Another critical use case of the HiL simulator is the generation of synthetic data: These synthetic data sets generated in the simulation environment are crucial for developing perception algorithms. The theoretically unlimited synthetic data allows the creation of a diverse data set that includes a wide range of traffic patterns and weather conditions and further enables the adaptation to different environments. Additionally, hazardous scenarios can be simulated and included in the data set. Since the ground truth positions of all objects in the simulation are known, the labor-intensive and often manual labeling of real-world data is not needed for synthetic data.

Fig. 6 depicts our HiL simulator architecture. Table 4 outlines the specifications. The GPU server runs the

[‡]<https://www.cohdawireless.com/solutions/hardware/mk5-obu/>

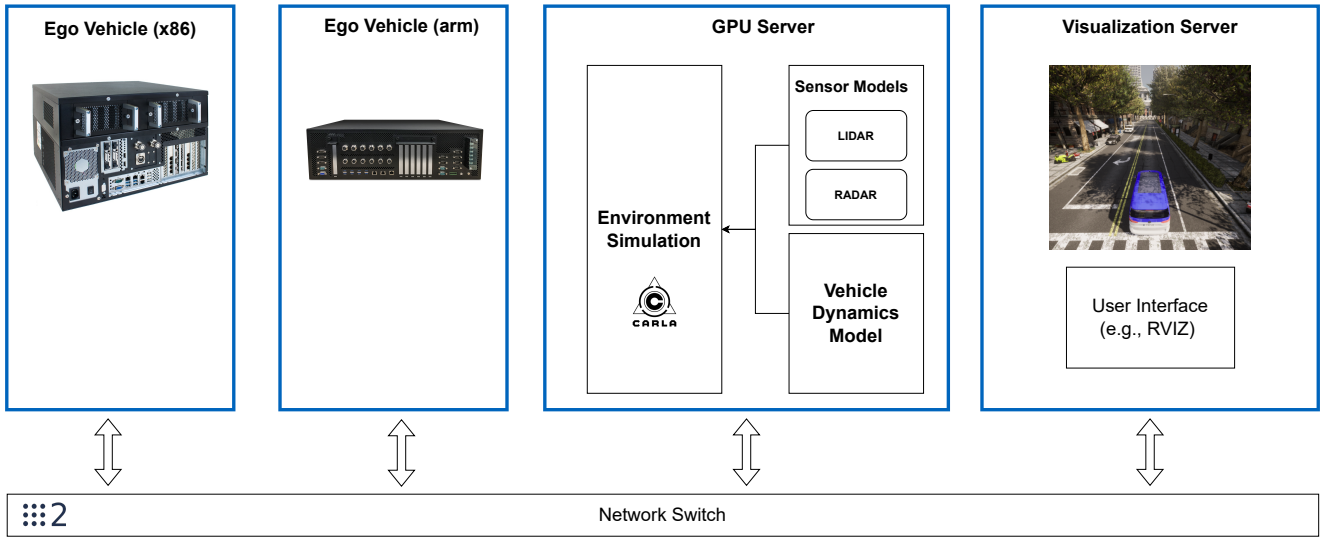


Figure 6. Overview about the HiL simulation setup.

Table 4. Specification of the components of the HiL simulator.

Server	CPU	RAM	Storage	NVIDIA GPU
GPU	2x AMD EPYC 75F3, 3.5 GHz	16x 32 GB	1x 7.68 TB NVMe; 2x 3.84 TB SAS	2x A40 48 GB
Visualization	Intel Xeon E-2286G, 4.0 GHz	4x 8 GB	1x 1 TB NVMe	2x A2000 12 GB

environment simulation, which includes virtual sensor models to generate synthetic sensor data and a vehicle dynamics model to simulate a sophisticated vehicle physics representation. The AV software runs on the vehicle computers (x86, ARM), which have the same interfaces as in the real vehicle. The ADLINK AVA Developer platform serves for the efficient development of code for arm-based CPUs. It is comparable to the AVA API but has a lower number of cores (32) and clock rate (1.5 GHz). The visualization server is used as input to control the other servers and the AV software stack. Furthermore, it displays the graphical output of the environment simulation and AV software states. All four compute platforms are connected via the network switch and communicate via ROS2.

3.6 Data Center

The *EDGAR* data center consists of data storage and computing servers. The data storage contains recorded sensor data from real-world test drives and simulations. The computing servers provides computing servers for data access management, continuous integration (CI), SiL, training neural networks, and performing data analysis.

We equipped the data center infrastructure with the servers listed in Table 5. The storage is separated into price-efficient hard drive disk (HDD) and latency-efficient solid-state drive (SSD) storage. The HDD storage is used as the main storage component of the data, whereas the SSD storage is used for frequently-used data provided on demand for computation tasks. Additionally, we have separate servers for CI tasks on different chips (x86, ARM), SiL, GPU-intensive tasks, and storage. The storage servers are integrated into an existing Ceph (Weil et al. 2006) cluster, which provides redundancy for hardware failures. The total amount of usable storage capacity is approximately for the HDD storage 2 PB and for the SSD storage 210 TB. Approximately 43 % of the capacity

is used by the Ceph cluster for redundancy. Additionally, we back up our raw data at the Leibnitz Supercomputing Centre (LRZ).

Our data center aims to provide captured data for the development process in two stages:

First, we provide the raw recorded data in rosbags. These can be used for scenario replay, post-test scenario analysis and scenario-oriented development.

Second, we extract and preprocess data from the available sensors and actuators embedded in the vehicle. This information collection includes images, point clouds, IMU and GPS readings, and CAN messages. To present the data systematically and structured, we organize it into a relational database, similar to the NuScenes dataset (Caesar et al. 2020). The architecture of this relational database is shown in Fig. 7.

Our top element is the *ride*. It resembles a real-world ride while simultaneously recording raw data. Each *ride* has a *calibrated sensor* table associated with it, with the intrinsic and extrinsic calibration matrices of the sensors. Similarly, each *ride* gets assigned a *map*. The ride is further divided into *scenes* of specific duration, which are tagged to classify the situations of interest. Within each *scene*, the time stamps for which all sensors have valid measurements are defined as a *sample*. The *sample data* are the measurements within the time window of the sample; each *sample data* has an attribute indicating which sensor recorded the sample. Finally, for each *sample*, an *ego pose* for the vehicle is also measured.

The tagging interface employed to label each recorded scene on an abstract level is depicted in Fig. 8 and deployed within the vehicle. A hierarchical approach was chosen for a fast and efficient labeling process. Each tag is assigned to a group and a category, while only relevant groups are displayed depending on the former selection. Furthermore, some tags, e.g., the sensor modalities or the vehicle speed,

Table 5. Specification of the components of the data center.

Name	Qty	CPU	RAM	Storage	GPU
SiL	1	2x AMD EPYC 75F3, 2.95 GHz	16x 32 GB	1x 7.68 TB NVMe; 2x 3.84 TB SAS	–
x86 CI	1	2x Intel Xeon Platinum 8362, 2.8 GHz	16x 16 GB	1x 7.68 TB NVMe; 2x 3.84 TB SAS	2x A40 48 GB
ARM CI	1	1 x Ampere Altra Max, M128-30, 3.0 GHz	2x 64 GB	2x 7.68 TB NVMe; 2x 0.96 TB SAS	1x A16 64 GB
MAC CI	1	1 x M2 Pro + 16-Core Neural Engine	32 GB	4x 4 TB SSD	19-Core GPU
GPU	1	2x AMD EPYC 9474F, 3.6 GHz	16x 128 GB	3x 7.68 TB NVMe	2x A100 80 GB
HDD	25	2x AMD EPYC 7252, 3.1 GHz	16x 8 GB	2x 1.92 TB NVMe; 12x 12 TB SAS	–
SSD	3	2x AMD EPYC 7313, 3.0 GHz	12x 16 GB	16x 7.68 TB NVMe; 2x 1.92 TB NVMe	–

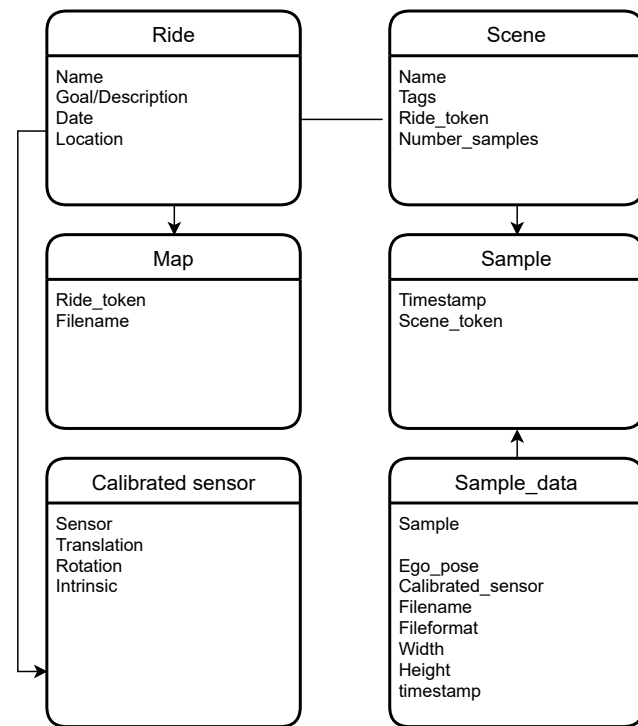
are automatically selected based on the information in the recorded rosbag.

4 System Design

We now present the overall network design of the vehicle, which includes all aforementioned components (4.1). Moreover, the driving modes to run the vehicle are introduced (4.2).

4.1 Network

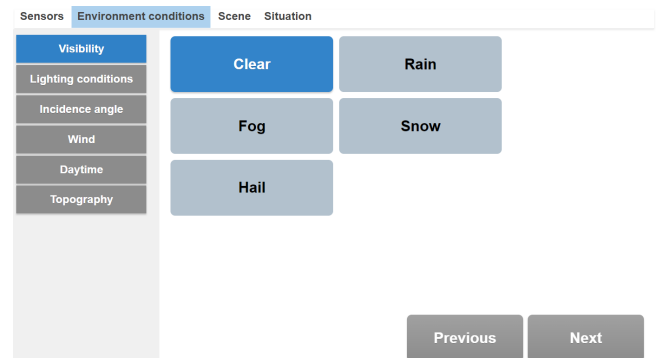
The network as shown in Fig. 9 comprises the environmental sensors, antennas, HPCs, and actuator interfaces. The mobile internet connection of the vehicle is established via the 5G antenna and the network router, which creates a VPN to all components in the vehicle to keep them in an isolated network. Both GPS antennas are input to the GPS-IMU system. However, one of the antennas is split and is also used as a reference clock of the PTP grandmaster. To synchronize the time of the GPS-IMU-system and the PTP grandmaster an additional PPS signal is sent to the grandmaster. The GM sends its time as a master time to the network switch, which distributes it to all sensors and computers.

**Figure 7.** Entity-Relationship Diagram.

The core element of the system is the network switch, which receives all sensor data, from the AV sensors and the series sensors, and passes them via 40 Gbit s⁻¹ Ethernet to the two HPCs. The switch, as outlined, operates as a TC, which allows for the exchange of PTP messages and updating their residence time. In addition, ultrasonic, RADAR, and camera are received via CAN. The AV computers output a CAN signal to actuate the vehicle. There are interfaces for the steering wheel, throttle and brake pedal, gearbox, and turn indicator, among others.

For an IVN, we must also validate that network packets arrive at their destination within pre-defined time bounds. Currently, no time bounds are ensured, but the system design allows for such guarantees, e.g., using the AVB/TSN features of the switch. The traffic prioritization over other traffic ensures Quality of Service (QoS) for higher priority traffic. This is especially important as combining all of the sensor data generates large throughput, which, without proper policing, can either overload the network or result in delays of high-priority/real-time traffic. The requirements on IVN were defined by the AVNU alliance (Pannell 2019) and categorized to Stream Reservation (SR) classes. The highest priority traffic belonging to the SR Class A requires a delay of less than 2 ms and jitter of less than 125 μs over seven hops (Pannell 2019).

To understand what TSN configurations are required, we plan to collect the various data feeds from the sources. Therefore, the selected sensors and other components support PTP, allowing for precise timestamping of the packets, thus, enabling accurate traffic pattern analysis and data fusion on the application layer. As a result, we are developing a cyber-physical twin containing the same network components to understand the impact of the various data streams from all sensor components in the network. To

**Figure 8.** Tagging interface with categories displayed in the top navigation bar, groups on the left side, and tags in the center of the screen.

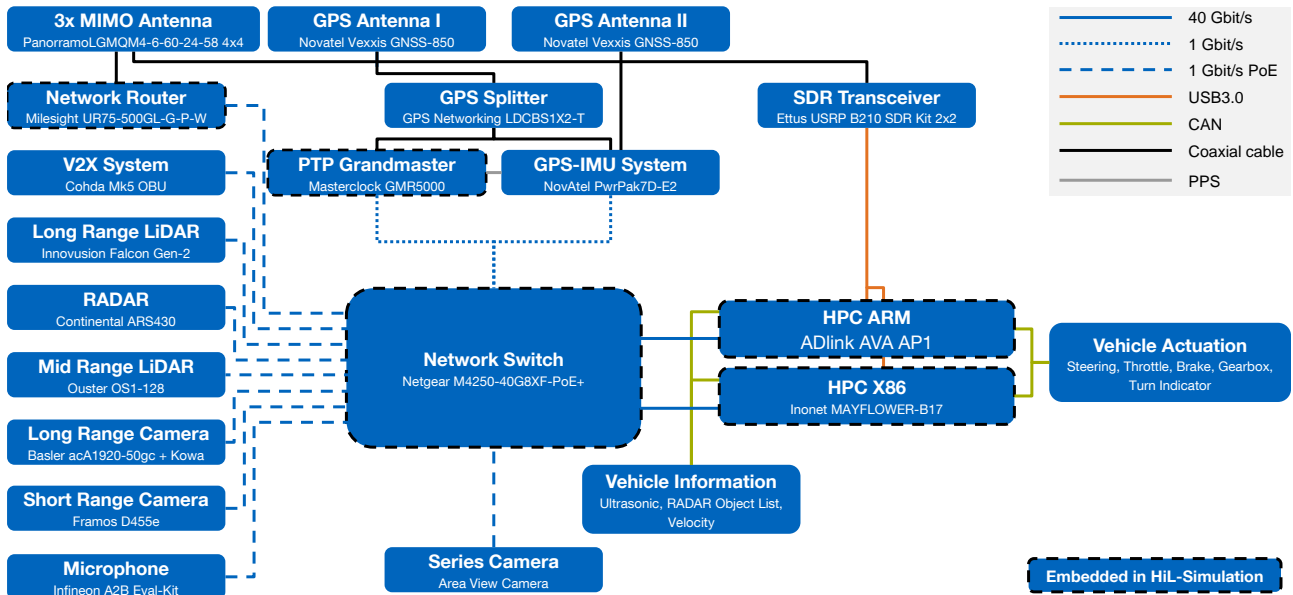


Figure 9. Network setup of the *EDGAR* platform comprising sensors, network switch, HPCs, and vehicle interfaces. For the sake of simplicity, the gateway between the series sensors and the AV hardware and the gateway to the actuators are not shown in the figure. In addition, the components embedded into the HiL simulation are shown.

offer more versatility, the twin not only contains the sensors as placed inside of the vehicle but also enables the data replay or modification of the data streams. Such an approach allows the simulation of additional scenarios that might not be present during the actual operation of the vehicle but might occur in various edge cases. The underlying network should be robust enough to handle such sudden changes.

Finally, in future iterations of autonomous vehicles, we will face the Vehicle-to-X scenarios in which various road traffic participants exchange data. The data must be precisely timestamped to enable relevance to other parties based on its freshness. Overall, the cyber-physical digital twin allows the assessment of additional behavior enabled by the selected components that allow precise timestamping and generate various traffic flows.

4.2 Driving Modes

The vehicle can run in four different modes, which are:

1. **Series Vehicle:** In this mode, the additional AV hardware is disconnected from the power supply and electronically separated from both series sensors and actuators.
2. **Measurement driving:** All actuator interfaces are electronically separated, but the AV sensors and the HPCs are enabled. Thus the mode can be used for data recording or running the software in ghost mode.
3. **Autonomous mode:** Lateral and longitudinal control is done by the software with limits of maximum speed, longitudinal acceleration and deceleration, lateral acceleration, and steering rate. This mode is used for test runs on public roads. The mode is implemented so that the safety driver can overrule steering, brake, and acceleration commands manually.
4. **High-dynamic mode:** This mode is used in testing areas only. This mode does not have limitations on longitudinal acceleration and deceleration and lateral

acceleration on the software side. Thus, speeds up to 130 km h^{-1} are possible, and the maximal steering rate can be used.

5 Digital Twin

Based on the autonomous vehicle setup presented in Section 3 and the system designed in Section 4, a digital twin is created to align the vehicle characteristics in the virtual and real environment. The digital twin comprises the three aspects of the vehicle dynamics model (5.1), replication of the sensor setup (5.2), and replication of the network setup (5.3).

5.1 Vehicle Dynamics

An appropriate vehicle dynamics model is essential for the virtual development and validation of motion planning and control algorithms. Various models, such as single-track, double-track, multi-body models, and finite element simulations, exist to capture vehicle dynamics (Guiggiani 2014). However, selecting the right model involves balancing complexity and efficiency. We adopt a dynamic nonlinear single-track model to account for essential dynamic effects, considering the combined slip of lateral and longitudinal tire forces, rolling resistance, and aerodynamic effects. To simulate lateral tire forces accurately, we use the Pacejka Magic Formula (Pacejka and Besselink 1997).

Validating the chosen model with real-world data and identifying parameter values are crucial for ensuring accuracy and reliability. We measure some parameters, including the position of the center of gravity and vehicle mass. We conduct steady-state circular driving behavior tests compliant with ISO 4138 (ISO 2021) to identify further parameters. Our focus is on the constant steering-wheel angle approach, and we employ two variations: discrete- and continuous speed increase tests. We collect motion and steering data from the GPS-IMU, Correvit, and VW Series

Table 6. Identified single track parameters.

	Value	Unit	Description
l	3.128	m	Wheelbase
l_f	1.724	m	Front axle to center of gravity
l_r	1.247	m	Rear axle to center of gravity
m	2,520	kg	Vehicle mass
I_z	13,600	kg m^2	Moment of inertia in yaw
ρ	1.225	kg m^{-3}	Air density
A	2.9	m^2	Cross-sectional frontal area
c_d	0.35		Drag coefficient

Table 7. Pacejka tire model parameters.

Parameter	Front	Rear	Description
B	10	12.4	Stiffness factor
C	1	1.8	Shape factor
D	$1.1 \cdot F_{z,f}$	$2.1 \cdot F_{z,r}$	Peak value
E	-5	-5	Curvature factor

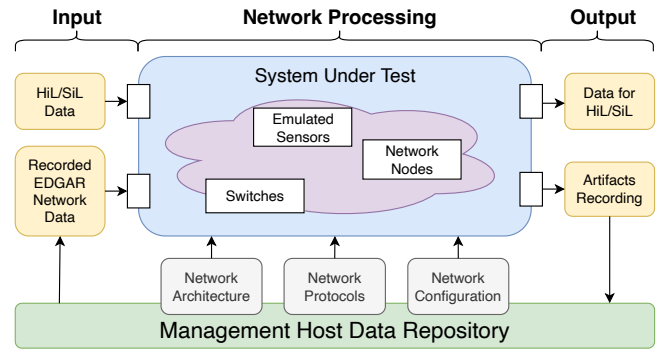
sensors. To cover both low- and high-velocity ranges, we conduct tests at velocities from 5 km h^{-1} up to 130 km h^{-1} , with steering wheel angles ranging from 45° to 540° in both turning directions. Under normal circumstances, i.e., clear weather, negligible wind speed, and an outside temperature of 23°C , we use Bridgestone 235/50R18 101H summer tires. The main single-track and tire model parameters are listed in Table 6 and 7, respectively, where $F_{z,\{f/r\}}$ represents the vertical static tire load at the front and rear axles.

5.2 Environment Sensors

For synthetic data generation, perception algorithm development, and validation tests, the exact replication of the sensor setup described in Section 3.2 is another important aspect of the digital twin. The position and orientation of each sensor are measured in the reference system of the middle of the rear axle. The specifications of the sensors (range, FOV, resolution) are given by the manufacturers. All parameters can be found in the repository. Based on this data, a 3D-model of the VW Multivan is equipped with the sensors. The respective sensor models for each sensor modality are taken from given open source solutions.

Sensor models can be separated into three main categories: high-, medium- and low-fidelity models. Low and medium-fidelity models primarily rely on ground-truth object lists to generate sensor data or simulate the sensor behavior. High-fidelity sensor models aim to simulate the underlying physical processes and their interaction with an available 3D environment and allow for higher data quality at the price of higher computational resource demand (Schlager et al. 2020).

With open-source simulation environments for automated driving based on established game engines like UnrealEngine 4.26 (Dosovitskiy et al. 2017) or Unity (TierIV 2023), the included camera models represent the state of the art to generate camera data. High-fidelity lidar and radar models rely on ray casting to simulate electromagnetic wave propagation. The available RobotecGPULidar allows the simulation of solid state and mechanical lidars via customizable lidar patterns (Robotec.AI 2023). High-fidelity radar simulations currently only exist as stand-alone developments (Holder

**Figure 10.** EnGINE (Rezabek et al. 2022a) components for cyber-physical twin of EDGAR.

2021; Thieling et al. 2021). It is however possible to implement a high-fidelity radar in open-source simulation environments. Microphone sensor models are currently not part of any open-source simulation framework for autonomous driving. Based on these given open source implementations further implementations of sensor models are intended to iteratively improve the digital replication of our sensor setup.

5.3 Network

Another aspect is validating and enhancing the underlying network supporting communication between system components such as sensors or the HPCs. The system must be robust and ensure deterministic data delivery under strict timing constraints. As mentioned in Section 4.1, the system is designed with a cyber-physical digital twin in mind. To better understand the required network architecture and design, we intend to use the EnGINE Framework (Rezabek et al. 2022a; Bosk et al. 2022) combined with artifacts obtained from real-world EDGAR testing.

The EnGINE framework is built using commodity off-the-shelf (COTS) hardware combined with open-source software solutions and enables verification of various network architectures and designs. It supports the generation of synthetic traffic patterns and replay of collected packet traces in an experimental setup, built as shown in Fig. 10. EnGINE also enables AVB traffic shaping and PTP time synchronization, further supporting other IEEE 802.1Q Time-Sensitive Networking standards (IEEE 2022) relevant for AV, e.g., IEEE 802.1Qav and Qbv standards. Beyond its capability of serving as a HiL system representing a form of a cyber-physical twin, the framework is extended using simulation (Bosk et al. 2023) based on the OMNeT++ discrete-event simulator. In this way, EnGINE can also serve as a SiL tool, enabling simultaneous execution of hardware-based and simulated experiments using a single configuration.

As a first step, using EnGINE we can build an exact representation of the network used within EDGAR shown in Fig. 9 centered around the Netgear M4250 network switch. The real-world sensors will be emulated using collected artifacts and COTS hardware devices. Such an approach improves the flexibility of the experimental environment while maintaining its realism and allows us to verify different protocols and the network configuration of EDGAR.

With its flexibility, EnGINE can serve as a platform to verify and improve *EDGAR*'s network and its configuration. The framework will allow us to focus on fulfilling the QoS requirements of various data streams by employing adequate TSN traffic shaping and policing mechanisms, beyond PTP time synchronization. With an understanding of the expected traffic patterns, we can use EnGINE to define and test those traffic shapers' appropriate selection and configuration. For example, highly time-critical information would instead require the use of scheduling provided by the IEEE 802.1Qbv standard, while high-bitrate streams would benefit from the traffic shaping defined in the IEEE 802.1Qav standard. EnGINE will allow us to define these correlations and ensure that *EDGAR*'s IVN can support all QoS requirements of the interconnected devices.

In the future, EnGINE will also enable us to come up with novel network architectures, and designs can then be developed using a combined HiL and SiL approaches. Using the framework's simulation extension, network topologies and device placements, beyond what is currently available and deployed in *EDGAR*, can be initially evaluated in a SiL setup. Such an approach can also enable further system optimization and shift focus toward the reliability and resilience of the IVN. These can later be properly validated on the physical EnGINE setup before any changes to the AV architecture of *EDGAR* are considered.

6 Development Workflow

The hardware setup presented in the previous sections needs to be applied in a suitable development workflow, which we present subsequently. A schematic overview of this workflow is shown in Fig. 11.

The feature development of our research covers aspects of every part of the autonomous software. The overall software architecture, into which the features are integrated, is *Autoware Universe* (Kato et al. 2018). Using this architecture, the developed code can be directly re-used with other research institutions, and the power of the open-source community significantly increases our pace of development.

The developed features and the composed overall software are first evaluated in unit tests and 2D SiL-simulations. These tests are part of the CI/CD toolchain, which is executed when code is committed. In addition, the tests are also executed in automated cloud-based scenario replays. Thereby, it is ensured that the software can be built and launched properly. Besides, the selection of standardized scenarios for the SiL-simulations allows us to track the progress of the overall software performance. Recorded sensor data are used to evaluate the performance of the perception modules. The motion planning benchmark framework CommonRoad is used as a scenario source to evaluate prediction and planning modules (Althoff et al. 2017). It was chosen due to the diversity of more than 16,000 synthetic and real scenarios, which allows an objective evaluation of the implemented functions.

The closed-loop full software stack simulation is the last step of the virtual test workflow. The software is deployed to the target computing platform and runs in a 3D environment, i.e., all parts of the software are included in the tests.

After the software passes the SiL- and HiL-test, the software is tested in real-world scenarios. To get as many insights as possible, our approach is to test the software in edge cases, i.e., at the limit of its capabilities. This contradicts a high record in the distance without disengagement, which is a common measure of the performance of the AV software in the state of the art. However, the efficiency of our test procedure, in terms of new insights about the performance of our software per driven kilometer, is very high with this edge-case-driven approach.

The next step after the tests are conducted is data management. The selection of which data should be uploaded focuses on abnormal events. These events comprise scenarios the software cannot solve, which are not covered by the simulation environment or are underrepresented in the data set for further development. From these abnormal events, either 2D scenarios are extracted in case there are complex interactive scenarios that challenge the decision-making and motion planning algorithms, or in case of challenges to perceiving the environment, the data is passed to the 3D HiL simulation.

7 Conclusion

A holistic platform for autonomous driving research is introduced. The core element is our research vehicle *EDGAR* and its digital twin, a virtual duplication of the vehicle. The vehicle is equipped with a multi-modal state of the art sensor setup, HPC platforms with different chip technologies, and fully accessible actuator interfaces. Its digital twin comprises vehicle dynamic models and sensor and network duplication for consistency between virtual and real-world testing. To the best of our knowledge, this is the first publicly available digital twin of an autonomous road vehicle. It ensures consistency between virtual and real-world tests, facilitates deployment, and reduces new software features' integration effort. All of these aspects boost the development of AV software stacks. The real and virtual vehicles embedded in the presented development workflow with a multi-stage simulation and testing approach and a large-scale data center. The proposed workflow covers the full process from feature development up to full-stack real-world tests.

Future work will tackle three central aspects. At first, we will validate the efficacy of our development process. It shall be investigated if the validation framework is able to prove the functionality on an algorithm, module, and overall software level. Our goal is to continuously improve the virtual validation stages by comparing the real-world performance of the software with the evaluation at the different simulation stages. Incomplete simulation behavior shall be corrected based on real-world observations. Thus, our digital twin will be continuously improved. Second, based on the introduced research platform, the development of new module software features, simulation models, evaluation frameworks, and software stack optimization is intended. In contrast to other works, our developed methods will always be validated within the whole software stack to analyze the dependencies and performance in a full stack. Lastly, we aim to create a large-scale urban, multi-modal data set. With a focus on edge cases such as adverse weather conditions and abnormal behavior of traffic participants and

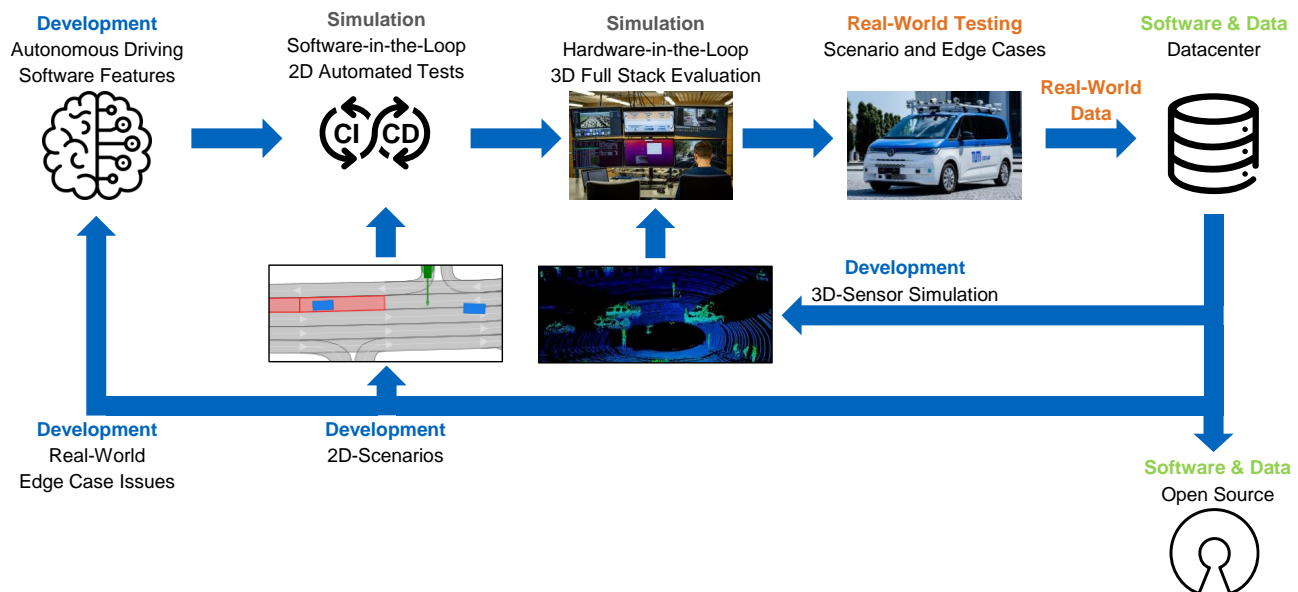


Figure 11. Development Workflow for *EDGAR*.

using auto-labeling and anomaly detection tools, we want to achieve a diverse data set to foster future research and software development.

All parts of our developed software and all collected data will be published open-source to share the gained knowledge and insights with the research community to accelerate the progress in autonomous driving research.

Contributions

As the first author, Phillip Karle initiated the idea of this paper, created the overall structure, and essentially contributed to all sections of the paper. The other authors contributed to the sections on the autonomous vehicle setup, system design, digital twin, development workflow, and the overall research projects. Johannes Betz contributed to essential parts of the paper and to the conception of the DFG proposal. Matthias Althoff led the DFG proposal for financing the vehicle; he had the idea to develop the digital twin. In addition, he developed the concept of sharing all data in a common data center and leads the CommonRoad project and its integration into EDGAR. Markus Lienkamp made an essential contribution to the conception of the DFG proposal. He supervised the setup of the vehicle and HiL and the conception of the development and validation workflow. He revised the paper critically for important intellectual content. He gave final approval of the version to be published and agreed with all aspects of the work. As a guarantor, he accepts responsibility for the overall integrity of the paper.

Acknowledgements

The vehicle was partly sponsored by a DFG grant (approval according to Art. 91b GG with DFG-number INST 95/1653-1 FUGG). In addition, the project is supported by the Bavarian Research Foundation (BFS), by MCube - Munich Cluster for the Future of Mobility in Metropolitan Regions, the German Research Community (DFG), the Federal Ministry for Economics Affairs and Climate Action, and by the research project ATLAS L4.

We gratefully thank our partners, Arm and the Xilinx University Program, for the donation of hardware platforms for our research environment.

Notes

1. (Thrun et al. 2006)
2. (Montemerlo et al. 2008; Levinson et al. 2011)
3. (Urmson et al. 2008)
4. (Ziegler et al. 2014)
5. (Grisleri and Fedriga 2010)
6. (Wei et al. 2013)
7. (Buechel et al. 2019; Kessler et al. 2019)
8. (Haselberger et al. 2022)
9. (Mehr et al. 2022)

References

- Althoff M, Koschi M and Manzing S (2017) Commonroad: Composible benchmarks for motion planning on roads. In: *2017 IEEE Intelligent Vehicles Symposium (IV)*. IEEE, pp. 719–726.
- Badue C, Guidolini R, Carneiro RV, Azevedo P, Cardoso VB, Forechi A, Jesus L, Berriel R, Paixão TM, Mutz F, de Paula Veronese L, Oliveira-Santos T and De Souza AF (2021) Self-driving cars: A survey. *Expert Systems with Applications* 165: 113816. DOI:<https://doi.org/10.1016/j.eswa.2020.113816>. URL <https://www.sciencedirect.com/science/article/pii/S095741742030628X>.
- Basantis A, Doerzaph Z, Harwood L and Neurauder L (2019) Developing a standardized performance evaluation of vehicles with automated driving features. *SAE International Journal of Connected and Automated Vehicles* 2(3). DOI:10.4271/12-02-03-0011. URL <https://doi.org/10.4271/12-02-03-0011>.
- Betz J, Betz T, Fent F, Geisslinger M, Heilmeier A, Hermansdorfer L, Herrmann T, Huch S, Karle P, Lienkamp M, Lohmann B, Nobis F, Ögretmen L, Rowold M, Sauerbeck F, Stahl T, Trauth R, Werner F and Wischnewski A (2023a) TUM autonomous motorsport: An autonomous racing software for

- the indy autonomous challenge. *Journal of Field Robotics* DOI: 10.1002/rob.22153. URL <https://doi.org/10.1002>.
- Betz T, Karle P, Werner F and Betz J (2023b) An analysis of software latency for a high-speed autonomous race car—a case study in the indy autonomous challenge. *SAE International Journal of Connected and Automated Vehicles* 6(3). DOI:<https://doi.org/10.4271/12-06-03-0018>. URL <https://doi.org/10.4271/12-06-03-0018>.
- Betz T, Schmeller M, Teper H and Betz J (2023c) How fast is my software? latency evaluation for a ros 2 autonomous driving software. In: *2023 IEEE Intelligent Vehicles Symposium (IV) Workshop*.
- Bosk M, Rezabek F, Abel J, Holzinger K, Helm M, Carle G and Ott J (2023) Simulation and Practice: A Hybrid Experimentation Platform for TSN. In: *International Federation for Information Processing (IFIP) Networking 2023 Conference (IFIP Networking 2023)*. Barcelona, Spain, p. 9.
- Bosk M, Rezabek F, Holzinger K, Marino AG, Fons F, Kane AA, Ott J and Carle G (2022) Methodology and Infrastructure for TSN-based Reproducible Network Experiments. *IEEE Access* DOI:10.1109/ACCESS.2022.3211969. URL <https://doi.org/10.1109/ACCESS.2022.3211969>.
- Broggi A, Bombini L, Cattani S, Cerri P and Fedriga R (2010) Sensing requirements for a 13,000 km intercontinental autonomous drive. In: *2010 IEEE Intelligent Vehicles Symposium*. pp. 500–505. DOI:10.1109/IVS.2010.5548026.
- Buechel M, Schellmann M, Rosier H, Kessler T and Knoll A (2019) Fortuna: Presenting the 5g-connected automated vehicle prototype of the project providentia. DOI:10.13140/RG.2.2.24402.91842.
- Burnett K, Yoon DJ, Wu Y, Li AZ, Zhang H, Lu S, Qian J, Tseng WK, Lambert A, Leung KY et al. (2022) Boreas: A multi-season autonomous driving dataset. *arXiv:2203.10168*.
- Caesar H, Bankiti V, Lang AH, Vora S, Liong VE, Xu Q, Krishnan A, Pan Y, Baldan G and Beijbom O (2020) nuscenes: A multimodal dataset for autonomous driving. In: *CVPR*.
- Campbell S, O'Mahony N, Krpalcova L, Riordan D, Walsh J, Murphy A and Ryan C (2018) Sensor technology in autonomous vehicles : A review. In: *2018 29th Irish Signals and Systems Conference (ISSC)*. pp. 1–4. DOI:10.1109/ISSC.2018.8585340.
- Carballo A, Lambert J, Monrroy A, Wong D, Narksri P, Kitsukawa Y, Takeuchi E, Kato S and Takeda K (2020) Libre: The multiple 3d lidar dataset. In: *2020 IEEE Intelligent Vehicles Symposium (IV)*. IEEE, pp. 1094–1101.
- Chakra R (2022) Exiting the simulation: The road to robust and resilient autonomous vehicles at scale. *arXiv:2210.10876*.
- Chen L, Li Q, Li M, Zhang L and Mao Q (2012) Design of a multi-sensor cooperation travel environment perception system for autonomous vehicle. *Sensors* 12(9): 12386–12404. DOI: 10.3390/s120912386. URL <https://www.mdpi.com/1424-8220/12/9/12386>.
- Cho H, Seo YW, Kumar BV and Rajkumar RR (2014) A multi-sensor fusion system for moving object detection and tracking in urban driving environments. In: *2014 IEEE International Conference on Robotics and Automation (ICRA)*. pp. 1836–1843. DOI:10.1109/ICRA.2014.6907100.
- Deliparaschos KM, Santha G, Fragonara LZ, Petrulin I, Zolotas AC and Tsourdos A (2020) A preliminary investigation of an autonomous vehicle validation infrastructure for smart cities. In: *2020 International Conference Mechatronic Systems and Materials (MSM)*. pp. 1–5. DOI:10.1109/MSM49833.2020.9201644.
- Dickmanns E (2002) The development of machine vision for road vehicles in the last decade. In: *Intelligent Vehicle Symposium, 2002. IEEE*, volume 1. pp. 268–281. DOI:10.1109/IVS.2002.1187962.
- Dosovitskiy A, Ros G, Codevilla F, López AM and Koltun V (2017) CARLA: An Open Urban Driving Simulator. In: *CoRL, Proceedings of Machine Learning Research*, volume 78. PMLR, pp. 1–16.
- Furgale P, Schwesinger U, Rufli M, Derendarz W, Grimmert H, Mühlfellner P, Wonneberger S, Timpner J, Rottmann S, Li B, Schmidt B, Nguyen TN, Cardarelli E, Cattani S, Brünig S, Horstmann S, Stellmacher M, Mielenz H, Köser K, Beermann M, Häne C, Heng L, Lee GH, Fraundorfer F, Iser R, Triebel R, Posner I, Newman P, Wolf L, Pollefeys M, Brosig S, Effertz J, Pradalier C and Siegwart R (2013) Toward automated driving in cities using close-to-market sensors: An overview of the v-challenge project. In: *2013 IEEE Intelligent Vehicles Symposium (IV)*. pp. 809–816. DOI:10.1109/IVS.2013.6629566.
- Gao J, Wu W and Aktouf OEK (2022) Adequate testing unmanned autonomous vehicle systems - infrastructures, approaches, issues, challenges, and needs. In: *2022 IEEE International Conference on Service-Oriented System Engineering (SOSE)*. pp. 154–164. DOI:10.1109/SOSE55356.2022.00025.
- Geyer J, Kassahun Y, Mahmudi M, Ricou X, Durgesh R, Chung AS, Hauswald L, Pham VH, Mühlegg M, Dorn S et al. (2020) A2d2: Audi autonomous driving dataset. *arXiv:2004.06320*.
- Grisleri P and Fedriga I (2010) The brave autonomous ground vehicle platform. *IFAC Proceedings Volumes* 43(16): 497–502. DOI:<https://doi.org/10.3182/20100906-3-IT-2019.00086>. 7th IFAC Symposium on Intelligent Autonomous Vehicles.
- Guiggiani M (2014) *The Science of Vehicle Dynamics*. Springer Netherlands. DOI:10.1007/978-94-017-8533-4. URL <https://doi.org/10.1007/978-94-017-8533-4>.
- Haselberger J, Pelzer M, Schick B and Müller S (2022) Jupiter – ros based vehicle platform for autonomous driving research. In: *2022 IEEE International Symposium on Robotic and Sensors Environments (ROSE)*. pp. 1–8. DOI:10.1109/ROSE56499.2022.9977434.
- Hatch R (1991) Instantaneous ambiguity resolution. In: Schwarz KP and Lachapelle G (eds.) *Kinematic Systems in Geodesy, Surveying, and Remote Sensing*. New York, NY: Springer New York. ISBN 978-1-4612-3102-8, pp. 299–308.
- Hauer F, Schmidt T, Holzmüller B and Pretschner A (2019) Did we test all scenarios for automated and autonomous driving systems? In: *2019 IEEE Intelligent Transportation Systems Conference (ITSC)*. pp. 2950–2955. DOI:10.1109/ITSC.2019.8917326.
- Holder MF (2021) *Synthetic Generation of Radar Sensor Data for Virtual Validation of Autonomous Driving*. PhD Thesis, Technische Universität Darmstadt, Darmstadt.
- IEEE (2020) Ieee standard for a precision clock synchronization protocol for networked measurement and control systems. *IEEE Std 1588-2019 (Revision of IEEE Std 1588-2008)* : 1–499 DOI:10.1109/IEEESTD.2020.9120376.

- IEEE (2022) Ieee standard for local and metropolitan area networks—bridges and bridged networks. *IEEE Std 802.1Q-2022 (Revision of IEEE Std 802.1Q-2018)* : 1–2163 DOI:10.1109/IEEESTD.2022.10004498.
- ISO (2021) Passenger cars: steady-state circular driving behaviour: open-loop test methods (iso 4138: 2021, idt).
- Kato S, Tokunaga S, Maruyama Y, Maeda S, Hirabayashi M, Kitsukawa Y, Monrroy A, Ando T, Fujii Y and Azumi T (2018) Autoware on board: Enabling autonomous vehicles with embedded systems. In: *2018 ACM/IEEE 9th International Conference on Cyber-Physical Systems (ICCPs)*. IEEE, pp. 287–296.
- Kessler T, Bernhard J, Buechel M, Esterle K, Hart P, Malovetz D, Truong Le M, Diehl F, Brunner T and Knoll A (2019) Bridging the gap between open source software and vehicle hardware for autonomous driving. In: *2019 IEEE Intelligent Vehicles Symposium (IV)*. pp. 1612–1619. DOI:10.1109/IVS.2019.8813784.
- Leonard J, How J, Teller S, Berger M, Campbell S, Fiore G, Fletcher L, Frazzoli E, Huang A, Karaman S, Koch O, Kuwata Y, Moore D, Olson E, Peters S, Teo J, Truax R, Walter M, Barrett D, Epstein A, Maheloni K, Moyer K, Jones T, Buckley R, Antone M, Galejs R, Krishnamurthy S and Williams J (2008) A perception-driven autonomous urban vehicle. *Journal of Field Robotics* 25(10): 727–774. DOI:https://doi.org/10.1002/rob.20262. URL https://onlinelibrary.wiley.com/doi/abs/10.1002/rob.20262.
- Levinson J, Askeland J, Becker J, Dolson J, Held D, Kammel S, Kolter JZ, Langer D, Pink O, Pratt V, Sokolsky M, Stanek G, Stavens D, Teichman A, Werling M and Thrun S (2011) Towards fully autonomous driving: Systems and algorithms. In: *2011 IEEE Intelligent Vehicles Symposium (IV)*. pp. 163–168. DOI:10.1109/IVS.2011.5940562.
- Li R and Zhai R (2019) Estimation and analysis of minimum traveling distance in self-driving vehicle to prove their safety on road test. *Journal of Physics: Conference Series* 1168(3): 032101. DOI:10.1088/1742-6596/1168/3/032101. URL https://dx.doi.org/10.1088/1742-6596/1168/3/032101.
- Ligocki A, Jelinek A and Zalud L (2020) Brno urban dataset - the new data for self-driving agents and mapping tasks. In: *2020 IEEE International Conference on Robotics and Automation (ICRA)*. pp. 3284–3290. DOI:10.1109/ICRA40945.2020.9197277.
- Lin SC, Zhang Y, Hsu CH, Skach M, Haque ME, Tang L and Mars J (2018) The architectural implications of autonomous driving: Constraints and acceleration. *Proceedings of the Twenty-Third International Conference on Architectural Support for Programming Languages and Operating Systems* 53(2): 751–766. DOI:10.1145/3296957.3173191. URL https://doi.org/10.1145/3296957.3173191.
- Liu K, Zhang X, Arcaini P, Ishikawa F and Jiao W (2020) Leveraging test logs for building a self-adaptive path planner. In: *Proceedings of the IEEE/ACM 15th International Symposium on Software Engineering for Adaptive and Self-Managing Systems, SEAMS '20*. New York, NY, USA: Association for Computing Machinery. ISBN 9781450379625, p. 57–63. DOI:10.1145/3387939.3391606. URL https://doi.org/10.1145/3387939.3391606.
- Macedo DF, Guedes D, Vieira LF, Vieira MA and Nogueira M (2015) Programmable networks—from software-defined radio to software-defined networking. *IEEE communications surveys & tutorials* 17(2): 1102–1125.
- Maurer M, Behringer R, Dickmanns D, Hildebrandt T, Thomanek F, Schiehlen J and Dickmanns ED (1995) VaMoRs-P: an advanced platform for visual autonomous road vehicle guidance. In: *Mobile Robots IX*, volume 2352. International Society for Optics and Photonics, SPIE, pp. 239 – 248. DOI: 10.1117/12.198974.
- Mehr G, Ghorai P, Zhang C, Nayak A, Patel D, Sivashangaran S and Eskandarian A (2022) X-car: An experimental vehicle platform for connected autonomy research powered by carma. *IEEE Intelligent Transportation Systems Magazine* DOI:10.1109/MITS.2022.3168801.
- Montemerlo M, Becker J, Bhat S, Dahlkamp H, Dolgov D, Ettinger S, Haehnel D, Hilden T, Hoffmann G, Huhnke B, Johnston D, Klumpp S, Langer D, Levandowski A, Levinson J, Marcil J, Orenstein D, Paefgen J, Penny I, Petrovskaya A, Pflueger M, Stanek G, Stavens D, Vogt A and Thrun S (2008) Junior: The stanford entry in the urban challenge. *Journal of Field Robotics* 25(9): 569–597. DOI:https://doi.org/10.1002/rob.20258. URL https://onlinelibrary.wiley.com/doi/abs/10.1002/rob.20258.
- Pacejka H and Besselink I (1997) Magic formula tyre model with transient properties. *Vehicle system dynamics* 27(S1): 234–249.
- Pannell D (2019) Automotive Ethernet AVB Functional and Interoperability Specification. https://avnu.org/wp-content/uploads/2014/05/Auto-Ethernet-AVB-Func-Interop-Spec_v1.6.pdf. Last accessed on 2022-05-10.
- Pomerleau DA (1988) Alvin: An autonomous land vehicle in a neural network. *Advances in neural information processing systems* 1.
- Rezabek F, Bosk M, Paul T, Holzinger K, Gallenmüller S, Gonzalez A, Kane A, Fons F, Haigang Z, Carle G and Ott J (2022a) EnGINE: Flexible Research Infrastructure for Reliable and Scalable Time Sensitive Networks. *Journal of Network and Systems Management* 30(4): 74. DOI:10.1007/s10922-022-09686-0. URL https://doi.org/10.1007/s10922-022-09686-0.
- Rezabek F, Helm M, Leonhardt T and Carle G (2022b) PTP Security Measures and their Impact on Synchronization Accuracy. In: *18th International Conference on Network and Service Management (CNSM 2022)*. Thessaloniki, Greece.
- RobotecAI (2023) Robotec GPU Lidar. https://github.com/RobotecAI/RobotecGPULidar.
- SAE (2021) Taxonomy and definitions for terms related to driving automation systems for on-road motor vehicles. *Ground Vehicle Standard J3016_202104Revised*.
- Schlager B, Muckenhuber S, Schmidt S, Holzer H, Rott R, Maier FM, Saad K, Kirchengast M, Stettinger G, Watzenig D and Ruebsam J (2020) State-of-the-art sensor models for virtual testing of advanced driver assistance systems/autonomous driving functions. *SAE International Journal of Connected and Automated Vehicles* 3(3): 233–261.
- Siwek P (2021) Analysis of microphone use for perception of autonomous vehicles. In: *2021 25th International Conference on Methods and Models in Automation and Robotics (MMAR)*. pp. 173–178. DOI:10.1109/MMAR49549.2021.9528431.

- Souza V, Cruz R, Silva W, Lins S and Lucena V (2019) A digital twin architecture based on the industrial internet of things technologies. In: *2019 IEEE International Conference on Consumer Electronics (ICCE)*. pp. 1–2. DOI:10.1109/ICCE.2019.8662081.
- Tao J, Li Y, Wotawa F, Felbinger H and Nica M (2019) On the industrial application of combinatorial testing for autonomous driving functions. In: *2019 IEEE International Conference on Software Testing, Verification and Validation Workshops (ICSTW)*. pp. 234–240. DOI:10.1109/ICSTW.2019.00058.
- Taraba M, Adamec J, Danko M and Drgona P (2018) Utilization of modern sensors in autonomous vehicles. In: *2018 ELEKTRO*. pp. 1–5. DOI:10.1109/ELEKTRO.2018.8398279.
- Thieling J, Frese S and Roßmann J (2021) Scalable and physical radar sensor simulation for interacting digital twins. *IEEE Sensors Journal* 21(3): 3184–3192.
- Thorn E, Kimmel SC, Chaka M, Hamilton BA et al. (2018) A framework for automated driving system testable cases and scenarios. Technical report, United States. Department of Transportation. National Highway Traffic Safety Administration. URL <https://rosap.ntl.bts.gov/view/dot/38824>.
- Thrun S, Montemerlo M, Dahlkamp H, Stavens D, Aron A, Diebel J, Fong P, Gale J, Halpenny M, Hoffmann G, Lau K, Oakley C, Palatucci M, Pratt V, Stang P, Strohband S, Dupont C, Jendrossek LE, Koelen C, Markey C, Rummel C, van Niekerk J, Jensen E, Alessandrini P, Bradski G, Davies B, Ettinger S, Kaehler A, Nefian A and Mahoney P (2006) Stanley: The robot that won the darpa grand challenge. *Journal of Field Robotics* 23(9): 661–692. DOI:<https://doi.org/10.1002/rob.20147>. URL <https://onlinelibrary.wiley.com/doi/abs/10.1002/rob.20147>.
- TierIV (2023) Awsim. <https://github.com/tier4/AWSIM>.
- Urmson C, Anhalt J, Bagnell D, Baker C, Bittner R, Clark M, Dolan J, Duggins D, Galatali T, Geyer C et al. (2008) Autonomous driving in urban environments: Boss and the urban challenge. *Journal of field Robotics* 25(8): 425–466.
- Van Brummelen J, O'Brien M, Gruyer D and Najjaran H (2018) Autonomous vehicle perception: The technology of today and tomorrow. *Transportation Research Part C: Emerging Technologies* 89: 384–406. DOI:<https://doi.org/10.1016/j.trc.2018.02.012>. URL <https://www.sciencedirect.com/science/article/pii/S0968090X18302134>.
- Wei J, Snider JM, Kim J, Dolan JM, Rajkumar R and Litkouhi B (2013) Towards a viable autonomous driving research platform. In: *2013 IEEE Intelligent Vehicles Symposium (IV)*. pp. 763–770. DOI:10.1109/IVS.2013.6629559.
- Weil SA, Brandt SA, Miller EL, Long DD and Maltzahn C (2006) Ceph: A scalable, high-performance distributed file system. In: *Proceedings of the 7th symposium on Operating systems design and implementation*. pp. 307–320.
- Williams M (1988) Prometheus-the european research programme for optimising the road transport system in europe. In: *IEE Colloquium on Driver Information*. pp. 1/1–1/9.
- Yurtsever E, Lambert J, Carballo A and Takeda K (2020) A survey of autonomous driving: Common practices and emerging technologies. *IEEE access* 8: 58443–58469. DOI:10.1109/ACCESS.2020.2983149.
- Zhao D and Peng H (2017) From the lab to the street: Solving the challenge of accelerating automated vehicle testing.
- Ziegler J, Bender P, Schreiber M, Lategahn H, Strauss T, Stiller C, Dang T, Franke U, Appenrodt N, Keller CG et al. (2014) Making bertha drive—an autonomous journey on a historic route. *IEEE Intelligent transportation systems magazine* 6(2): 8–20.
- Zong W, Zhang C, Wang Z, Zhu J and Chen Q (2018) Architecture design and implementation of an autonomous vehicle. *IEEE Access* 6: 21956–21970. DOI:10.1109/ACCESS.2018.2828260.